

Acetone in the upper troposphere/lowermost stratosphere measured by the CARIBIC passenger aircraft: Distribution, seasonal cycle, and variability

Detlev Sprung¹ and Andreas Zahn¹

Received 31 March 2009; revised 15 January 2010; accepted 18 February 2010; published 17 August 2010.

[1] Mass-spectrometric measurements of acetone (CH_3COCH_3) have been performed monthly using a Lufthansa Airbus A340-600 passenger aircraft between February 2006 and December 2008. In total, 106 measurement flights (4 per month) were conducted between Germany and South America, North America, South Asia, and East Asia. Here measurements collected between 33°N and 56°N in the upper troposphere (UT) and lowermost stratosphere (LMS) at 9–12 km altitude are analyzed. By integrating data collected at 12 ozonesonde stations, ozone concentrations measured on flight are translated into a representative (mixing-based) altitude above the thermal tropopause. A strong seasonal variation of acetone occurs at the midlatitude tropopause with maxima of ~ 900 parts per 10^{12} vol (pptv) in summer and minima of ~ 200 pptv in midwinter. This seasonality propagates into the LMS in approximately 6 weeks with rapidly decreasing concentrations and increasing phase shifts reaching 2 km above the tropopause. Throughout the year, acetone and ozone are highly negatively correlated in the LMS with a mean linear correlation coefficient (R) of -0.93 . This linear relationship marks the O_3 -acetone-based extratropical tropopause mixing layer (exTL). A “stratospheric intrusion height of acetone” (Z_{acetone}) is defined that concurs with the vertical depth of the O_3 -CO-based exTL, namely, averaging ~ 2.2 km but with slightly lower values in winter. Probability density functions (PDFs) and the course of the seasonal variation of acetone relative to the tropopause are interpreted regarding the in-mixing and subsequent dispersion of acetone in the LMS.

Citation: Sprung, D., and A. Zahn (2010), Acetone in the upper troposphere/lowermost stratosphere measured by the CARIBIC passenger aircraft: Distribution, seasonal cycle, and variability, *J. Geophys. Res.*, 115, D16301, doi:10.1029/2009JD012099.

1. Introduction

[2] Acetone (CH_3COCH_3) is omnipresent in the troposphere and one of the most abundant oxygenated volatile organic compound (OVOCs) [Singh *et al.*, 1994, 1995]. As given in a budget analysis by Jacob *et al.* [2002, and references therein], the major sources of acetone are direct anthropogenic and biogenic emissions (terrestrial vegetation, grasslands, biomass burning); the decay of dead plant matter makes a small contribution. Minor sources of acetone are secondary production by atmospheric oxidation of biogenic precursors (particularly isoprene and others such as monoterpenes and methylbutenol) and anthropogenic low-number (C_3 to C_5) isoalkanes originating mainly from automobile fuel evaporation and natural gas exploitation. The oceans act as either sources or sinks, depending on light, microbial activity, and water temperatures [Wisthaler *et al.*, 2002; de Laat *et al.*, 2001; Warneke and de Gouw, 2001; Singh *et al.*, 2003]. Besides dry deposition to ocean and land surfaces, major

sinks are the reaction with OH, photodissociation in the UV [Folkins *et al.*, 1998; Wennberg *et al.*, 1998], and reaction with HO_2 at low temperatures in the upper troposphere/lowermost stratosphere (UT/LMS) [Hermans *et al.*, 2004, 2005; Cours *et al.*, 2007].

[3] Formerly, acetone photolysis was assumed to be the dominant precursor of HO_x ($\text{HO} + \text{HO}_2$) in the dry UT/LMS with H_2O mixing ratios of less than ~ 100 parts per 10^6 vol (ppmv) [Singh *et al.*, 1995, 2000; Wennberg *et al.*, 1998; Jaeglé *et al.*, 2001]. A more recent laboratory study on the quantum yield for the photolysis of acetone by Blitz *et al.* [2004] questions this picture. Subsequent model studies by Arnold *et al.* [2004, 2005] adjusted the loss rate of acetone and thus the relevant source of OH down by 60% near the ground and by 90% near the midlatitude tropopause. Arnold *et al.* [2005] scaled up the mean atmospheric (global) lifetime to ~ 35 d and reduced the global source strength to ~ 42.5 Tg a^{-1} . Their results further implied that the reaction with OH would be the dominant acetone sink. According to a comment by one of the (anonymous) reviewers of this paper, the GEOS-Chem model (used by the group of D.J. Jacob, http://map.nasa.gov/GEOS_CHEM.html, Jacob *et al.* [2002]), however, calculated over the same time a reduction of the global lifetime of acetone and of the global OH source strength by only 20%, to 18 d and ~ 80 Tg a^{-1} , respectively.

¹Karlsruhe Institute of Technology (KIT), Institute of Meteorology and Climate, Karlsruhe, Germany.

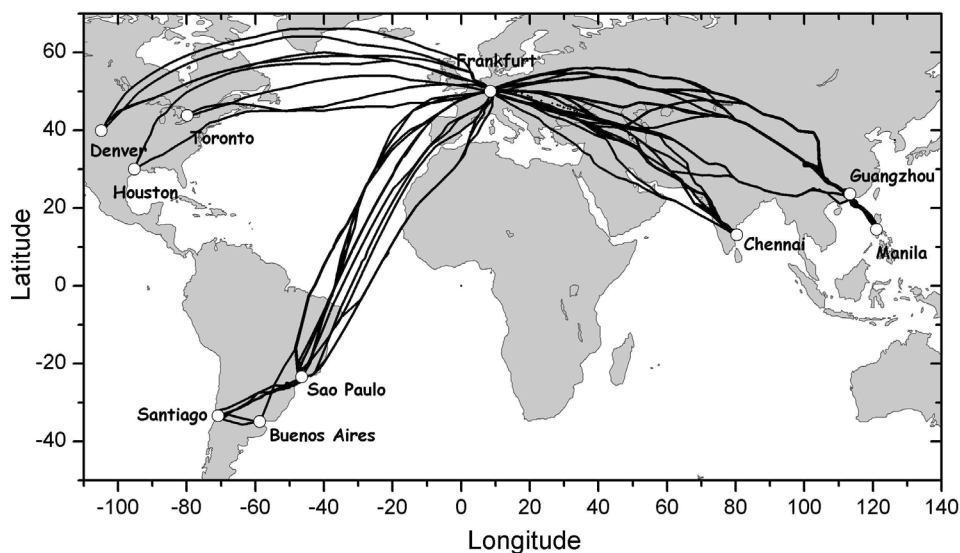


Figure 1. Civil aircraft for the regular investigation of the atmosphere based on an instrument container (CARIBIC) flight tracks between March 2005 and December 2008. All data collected north of 33°N are considered in the present analysis.

We conclude that the photolysis of acetone is still a poorly quantified OH source in the UT/LMS.

[4] Besides remaining a relevant precursor of HO_x, a sequestering of reactive nitrogen by the formation of peroxyacetyl nitrate occurs in the reaction chain after acetone photolysis [Singh *et al.*, 1995; Jaegle *et al.*, 1997].

[5] That the chemical (local) lifetime of acetone is weeks to months in the UT/LMS indicates its local concentration is determined by the actual partitioning between import of acetone and its precursors from lower altitudes, in situ production (usually weak), and the loss processes mentioned above.

[6] Besides first retrievals from infrared spectrometers onboard balloons [Remedios *et al.*, 2007] and satellites [Coheur *et al.*, 2007], precise acetone data from the UT/LMS have originated from research aircraft campaigns in the wake of Arnold and Hauck [1985]. In the Southern Hemisphere tropical midtroposphere to UT (8–12 km) mean values were ~350 parts per 10¹² vol (pptv), whereas ~650 pptv was detected in the Northern Hemisphere [Jacob *et al.*, 1996; Singh *et al.*, 2001, 2004]. Measurements in the midlatitude Northern Hemisphere show mixing ratios of 300–2000 pptv in the upper troposphere and 50–280 pptv in the lowermost stratosphere [Arnold *et al.*, 1986, 1997; Chatfield *et al.*, 1987; Singh *et al.*, 1995, 1997; Wohlfrom *et al.*, 1999; Fischer *et al.*, 2003; Kiendler and Arnold, 2003; Scheeren *et al.*, 2003; de Gouw *et al.*, 2004; Colomb *et al.*, 2006].

[7] More accurate observations of acetone in the UT/LMS are expected to contribute to a better understanding of its atmospheric budget and thus better quantification of its role in the oxidative cycle of the atmosphere. The data presented here originate from the first systematic and regular monitoring of acetone in the extratropical UT/LMS over a period of 3 years.

2. Experimental

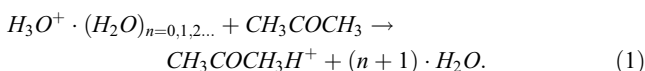
[8] CARIBIC (Civil aircraft for the regular investigation of the atmosphere based on an instrument container) involves

deployment of a flying laboratory, i.e., a modified airfreight container equipped with automated instruments for in situ and remote-sensing measurement as well as equipment for air sampling and aerosol particle collection. The container is installed each month in the cargo bay of a passenger aircraft (Lufthansa Airbus A340-600) and connected to a permanent air intake system underneath the aircraft [Brenninkmeijer *et al.*, 2005, 2007]. The acetone data presented here were collected at cruising altitudes between 300 and 200 hPa (9–12 km altitude) and between 33°N and 56°N from February 2006 to December 2008 (106 flights, ~720 h at flight level). See flight tracks in Figure 1.

[9] Sample air flows from the heated inlet system through a perfluoroalkoxy inlet line (~1 cm [3/8 in.] OD) inside the aircraft, kept at 30°C to the individual trace gas instruments. Acetone is measured using a proton-transfer-reaction quadrupole mass spectrometer (PTR-MS), described briefly by Brenninkmeijer *et al.* [2007].

[10] Our PTR-MS is a modified version of the commercially available instrument of Ionicon (Innsbruck, Austria). The fundamentals of the PTR-MS technique are given by Lindinger *et al.* [1998]. Hansel *et al.* [1998] describes the first application of a PTR-MS on research aircraft. For a review we refer to de Gouw and Warneke [2007]. The basics are summarized here.

[11] Water vapor is ionized in a hollow cathode providing H₃O⁺ primary ions that transfer their proton within a drift tube (reaction chamber, here at 2.8 hPa) to gases with proton affinities higher than that of water (most OVOCs); e.g., for acetone,



Primary and product ions (59 amu for acetone) enter a quadrupole mass spectrometer for detection with an electron multiplier. The ratio between product ions to H₃O⁺ primary

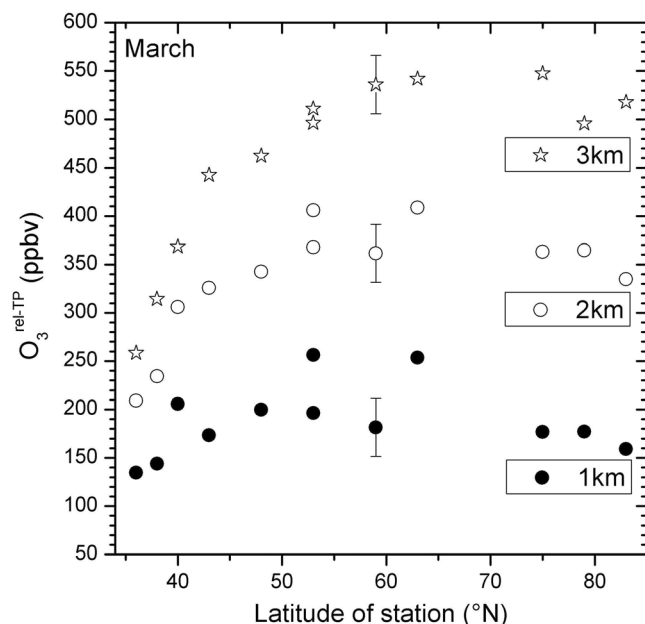


Figure 2. Monthly averaged ozone mixing ratio at distances of 1.0, 2.0, and 3.0 km above the thermal tropopause relative to the ozone mixing ratio at the thermal tropopause, as the average for all March values from 1980 to 1995. Data measured at 12 ozonesonde stations in the Northern Hemisphere between 114°W and 140°E from 1980 to 1995. These data (together with a description) were already reported by Logan [1999].

ions is proportional to the concentration of the respective trace gas. The isobaric species propanal, $\text{CH}_3\text{CH}_2\text{CHO}$ (an isomer of acetone), and glyoxal, $\text{CH}(\text{O})\text{CH}(\text{O})$, are also detected with the PTR-MS technique at $m = 59$ amu. However, because their atmospheric lifetimes are only in terms of hours [Williams *et al.*, 2001; Warneke and de Gouw, 2001], the concentrations of propanal and glyoxal are negligible in the UT/LMS.

[12] We determine the proportionality factor or sensitivity S by adding a calibration gas (Apel Riemer, USA; acetone mixing ratio: 500 parts per 10^9 vol (ppbv); given uncertainty: 5%) to the sample gas in ratios of $\sim 1:100$ and $\sim 1:200$. S typically is $120 \text{ cps ppbv}^{-1}$. From the difference between the measured signal and a background signal (at 59 amu), and from the sensitivity S determined by the calibration measurement, the actual acetone concentration is calculated. The background signal is determined by measuring zero air produced using a Pt catalyst (350°C). A mass spectrum (scanning 19 selected gases) lasts 60 s (~ 15 km at flight altitude); the integration time for the acetone measurement was 5 s corresponding to ~ 1.25 km at cruising altitude. Calibration and background measurements are performed once each hour. The background determines the detection limit of typically 20 pptv in the 5 s measurement time. The calibration gas concentrations are controlled in the laboratory by cross-checks with two identical gas standards that are about 1 and 2 years older, respectively. No changes occurred during the entire measurement period addressed here. The total uncertainty of the acetone data is $\sim 10\%$ above 200 pptv and ~ 20 pptv below 200 pptv.

[13] Ozone is measured using a homemade, very accurate UV photometer showing a precision of 0.3 ppbv or 0.3% (whatever is highest) at a measurement time of 4 s (or 1 km at flight altitude) and a total uncertainty of $\sim 1.5\%$ (dominated by the uncertainty of the O_3 absorption cross section at a wavelength of 254 nm).

3. Use of Ozone as Vertical Coordinate in the Lowermost Stratosphere

[14] A crucial topic of this paper is the better comprehension of the seasonally changing vertical profile of acetone at the transition from the upper troposphere into the lowermost stratosphere and a better quantification of the controlling processes. This will, *inter alia*, be done by interpreting the likewise measured ozone mixing ratio as measure for the altitude above the tropopause. For translating O_3 mixing ratios into a vertical scale above the tropopause, monthly mean vertical O_3 profiles observed at 12 stations north of 35°N are used. These ozonesonde data have already been presented by Logan [1999] and updated by Considine *et al.* [2008].

[15] As an example in Figure 2, these data are shown for the month March as difference of the O_3 mixing ratio at distances Z_{TP} of 1.0, 2.0, and 3.0 km above the thermal tropopause relative to the O_3 mixing ratio at the thermal tropopause; that is,

$$\text{O}_3^{\text{rel-TP}}(Z_{\text{TP}}, \text{month}) = \text{O}_3(Z_{\text{TP}}, \text{month}) - \text{O}_3(0, \text{month}). \quad (2)$$

[16] Although the data displayed in Figure 2 are, on average, based on only 36.8 ozone soundings per station, the differences between adjacent stations are modest. The scatter between adjacent stations decreases with height above the tropopause, most likely because of decreasing influence of tropospheric laminae and thus decreasing variability with increasing distance to the tropopause. A larger number of considered O_3 soundings, *i.e.*, better statistics, will likely result in weaker differences between adjacent stations. Besides this, a gradual dependence on latitude is obvious. That is, on time scales of a month, a certain O_3 mixing ratio is characteristic for a certain altitude above the tropopause.

[17] We now address the question how accurate we can estimate this distance relative to the tropopause. In Figure 2, at each distance above the tropopause an error bar is shown (at 59°N), which indicates maximum O_3 differences (ΔO_3) between adjacent stations at the respective altitude. Together with the O_3 mixing ratio $\text{O}_3^{\text{rel-TP}}$ (y axis, defined in equation (2)) and the distances above the tropopause $Z_{\text{TP}} = 1.0, 2.0,$ and 3.0 km, an uncertainty ΔZ_{TP} of the O_3 -derived altitude above the tropopause can be inferred; for example, at $Z_{\text{TP}} = 2.0$ km,

$$\Delta Z_{\text{TP}}(2.0 \text{ km}) = \frac{\Delta\text{O}_3}{\text{O}_3^{\text{rel-TP}}} \cdot Z_{\text{TP}} = \frac{30 \text{ ppbv}}{260 \text{ ppbv}} \cdot 2 \text{ km} = 231 \text{ m}. \quad (3)$$

As indicated in Table 1, at all altitudes considered, a certain O_3 mixing ratio can be translated to an altitude above the thermal tropopause with an uncertainty of 300–500 m.

[18] We have just demonstrated that the close relationship between O_3 and the altitude above the extratropical tropopause is valid for time scales of 1 month. But is this rela-

Table 1. Estimated Accuracy of the Representative (Mixing-Based) Altitude Above the Thermal Tropopause (TP) ΔZ_{TP} Derived From O_3 Data Collected at 12 Stations North of 35°N at Three Heights Above the TP

Distance Above TP, Z_{TP}^a (km)	O_3 Relative to TP, O_3^{rel-TP} (ppbv)	Variability, ΔO_3 (ppbv)	ΔZ_{TP} (Without Interannual Variability)		Interannual Variability of O_3 (%) ^b	ΔZ_{TP} (Total)	
			Relative (%)	Absolute (m)		Relative (%)	Absolute (m)
1.0	160	30	18.8	188	10	28.8	288
2.0	260	30	11.6	231	10	21.6	432
3.0	360	30	8.3	250	10	18.3	549

^aAltitude above the thermal tropopause, ΔZ_{TP} , both relative (%) and absolute (m) (see Figure 2).

^bBased on MOZAIC data [Thouret *et al.*, 2006].

tionship also valid for short time scales; i.e., is a certain O_3 mixing ratio (e.g., measured on board aircraft) characteristic for a certain altitude above the tropopause? Yes! We will now demonstrate why.

[19] Ozone is a transport tracer in the LMS owing to its long local chemical lifetime of ~ 1 year [Solomon *et al.*, 1985]. Its strong decrease from the LMS upper boundary, being the 380 K potential surface, to its lower boundary, being the extratropical tropopause [Holton *et al.*, 1995], is controlled by the dilution of descending O_3 -rich stratospheric air with inflowing O_3 -poor tropospheric air. This mixing process results in a steep vertical gradient of ozone and makes it to a potential measure of the altitude above the extratropical tropopause.

[20] Individual vertical ozone soundings usually show strong vertical fluctuations [Reid and Vaughan, 1991], and if ozone data from many vertical soundings are plotted together relative to the tropopause [see, e.g., Figure 4 by Pan *et al.*, 2004], a strong scatter appears above the tropopause. This variability is of course due to the strong horizontal layering of the atmosphere; i.e., air masses at different altitudes above the local tropopause can originate from many different locations and altitudes, as has been nicely visualized, e.g., in contour advection studies [Appenzeller *et al.*, 1996]. Ozone is a quasi-inert air component in the LMS and is passively transported with each air movement. On short time scales (days) and as indicated by the fluctuations in vertical soundings, ozone is certainly not a measure of the instantaneous altitude above the tropopause; it is, however, a measure of the mean altitude at which the sampled air mass had been the “last time” before sampling. This time is in the order of 1 to 2 weeks, i.e., just long enough to smooth the fluctuations of the vertical soundings. That is, the O_3 -derived altitude above the thermal tropopause describes a “representative altitude,” i.e., an altitude where the sampled air mass has on average been the last 1 to 2 weeks before sampling. One can also say that the O_3 -derived altitude above the thermal tropopause is a “mixing-based altitude” as it reflects the degree of mixing between two reservoirs, namely, between O_3 -poor UT air and O_3 -rich LMS air.

[21] A very similar reasoning is applied to the equivalent latitude where the potential vorticity is used to assign a sampled air mass to its mean or representative latitude of occurrence in the lowermost stratosphere [Butchart and Remsberg, 1986; Hegglin *et al.*, 2006].

[22] Besides the uncertainty inferred above, a further uncertainty comes along interannual variations of ozone in the LMS. The interpretation of O_3 data collected between 1994 and 2003 onboard the MOZAIC passenger aircraft resulted in maximum interannual variations of as much as

10–15% in the LMS [Thouret *et al.*, 2006]. Therefore, we estimate the total uncertainty of the O_3 -derived altitude above the tropopause to be 20% or ~ 400 m at $Z_{TP} = 2.0$ km (Table 1). A more sophisticated analysis of the O_3 -derived altitude above the tropopause is beyond the scope of this paper and will be presented in a future paper.

[23] The uncertainty of 20% is low compared with that for other parameters currently applied. For instance, the simple interpolation of the thermal tropopause from meteorological analyses to the latitude/longitude of the aircraft results in a much higher uncertainty, because the usually rapidly changing small-scale structures around the extratropical tropopause cannot be resolved by current models. For horizontally flying platforms such as passenger aircraft, which may cross the tropopause up to 20 times during a single flight, the coarse model resolution does not resolve tropopause features in sufficient detail. Finally, we emphasize again that the O_3 -based distance above the tropopause cannot be interpreted as instantaneous distance above the tropopause and thus should not be compared with the actual distance above the tropopause, e.g., that inferred from meteorological analyses.

[24] Practically, the O_3 -based altitude above the tropopause $Z_{TP}(O_3)$ for any O_3 mixing ratios is calculated in this study as follows.

[25] 1. Two ozonesonde stations, A and B, are identified as being located closest north and south of the CARIBIC sampling latitude.

[26] 2. The two ozone/altitude levels of both stations, which bracket the relevant CARIBIC O_3 mixing ratio, are identified, i.e., $O_3(Z_{TP}^1, A)$, $O_3(Z_{TP}^2, A)$, $O_3(Z_{TP}^1, B)$, $O_3(Z_{TP}^2, B)$.

[27] 3. The O_3 mixing ratios at both levels Z_{TP}^1 and Z_{TP}^2 at the CARIBIC sampling latitude are interpolated; i.e., for Z_{TP}^1

$$\begin{aligned} \overline{O_3}(Z_{TP}^1) &= \overline{O_3}^A(Z_{TP}^1) \\ &+ \frac{\overline{O_3}^B(Z_{TP}^1) - \overline{O_3}^A(Z_{TP}^1)}{\text{Latitude}^B - \text{Latitude}^A} (\text{Latitude}^{\text{CARIBIC}} - \text{Latitude}^A). \end{aligned} \quad (4)$$

[28] 4. A linear interpolation between these two mean ozone/altitude levels $\overline{O_3}(Z_{TP}^1)$ and $\overline{O_3}(Z_{TP}^2)$ finally results in the (representative) altitude at the considered O_3 mixing ratio.

[29] For instance, if we are interested in $Z_{TP}(O_3)$ at $O_3 = 440$ ppbv at 50°N in July, we search for the adjacent O_3 levels at the two adjacent ozonesonde stations (Hohenpeissenberg at 48°N and Goose Bay at 53°N) at July; calculate the two mean O_3 mixing ratios, i.e., 400 ppbv at 2.0 km and 458 ppbv at

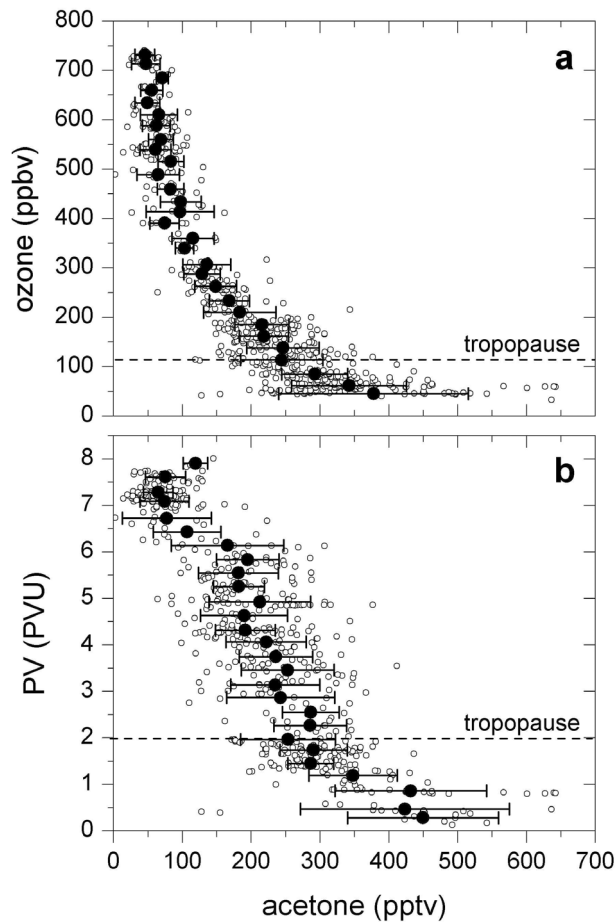


Figure 3. (a) Acetone versus ozone and (b) potential vorticity unit (PVU; $1 \text{ PVU} = 10^{-6} \text{ km}^2 \text{ kg}^{-1} \text{ s}^{-1}$) for a series of four flights conducted between 5 and 7 February 2007. Open circles indicate single measurements; solid dots indicate mean data averaged in O_3 and potential vorticity bins of $\sim 25 \text{ ppbv}$ and $\sim 0.25 \text{ PVU}$, respectively. Horizontal bars indicate 1σ variability.

3.0 km above the thermal tropopause (step 3); and linearly interpolate between the two levels (step 4):

$$Z_{TP}(440 \text{ ppbv}) = 2.0 \text{ km} + \frac{3.0 - 2.0}{458 - 400} \frac{\text{km}}{\text{ppbv}} (440 - 400) \text{ ppbv} = 2.69 \text{ km}. \quad (5)$$

That is, for each O_3 mixing ratio higher than the one at the thermal tropopause (e.g., 148 ppbv over Hohenpeissenberg in July), the altitude above the thermal tropopause can be derived.

4. Vertical Profile and Variability of Acetone Around the Midlatitude Tropopause

[30] Aircraft-based studies, primarily during recent years, discovered the existence of a mixing layer just above the extratropical tropopause. This layer is characterized by a continuous transition from the trace gas composition in the UT to that of background LMS air, i.e., air that had not recently been affected by in-mixing of tropospheric air

[Fischer et al. 2000; Hoor et al., 2002; Zahn et al., 2004; Pan et al., 2004; Hegglin et al., 2009]. In this extratropical tropopause transition layer (exTL) tracers of stratospheric air, e.g., O_3 , are closely but negatively correlated with (sufficiently long-lived) tracers of tropospheric air such as CO or acetone.

[31] First, we investigate and demonstrate the compact correlation between acetone and ozone in the exTL for our measurements. As an example, for a flight series on 5–7 February 2007 the acetone data are plotted versus the simultaneously measured O_3 mixing ratios (Figure 3a) and the ECMWF-derived PV values are interpolated to the latitude/longitude of the CARIBIC aircraft (Figure 3b; for data and description, see http://www.knmi.nl/samenw/campaign_support/CARIBIC/#LH).

[32] Three main differences can be identified: (1) The correlation between acetone and the in situ-measured O_3 concentration is much more compact compared to the correlation with the model-derived PV. The horizontal bars indicating the 1σ variability at the individual O_3 and PV levels are about a factor of two smaller for the O_3 -acetone correlation. (2) The mean profile (black circles) is much smoother for the O_3 -acetone correlation and its knee at $\text{O}_3 \sim 400 \text{ ppbv}$ nicely marks the top of the exTL, a feature that is not visible in the PV-acetone correlation. (3) The acetone background mixing ratio in the LMS of 50–100 pptv above $\text{O}_3 \sim 400 \text{ ppbv}$ is identifiable only in the O_3 -acetone profile. Figure 3 demonstrates that the in situ-measured O_3 mixing ratio is the more accurate tracer of the sampled air mass and thus more characteristic for the altitude above the tropopause (see discussion above) than is the (temporally and spatially) much more coarsely resolved model-derived quantity PV.

[33] In Figure 4 vertical acetone profiles observed during four flights in different seasons are depicted using the O_3 -based vertical-scale $Z_{TP}(\text{O}_3)$. The horizontal bars indicate the 1σ variability of acetone in the respective altitude bin having a vertical extension of $\sim 250 \text{ m}$. This variability almost

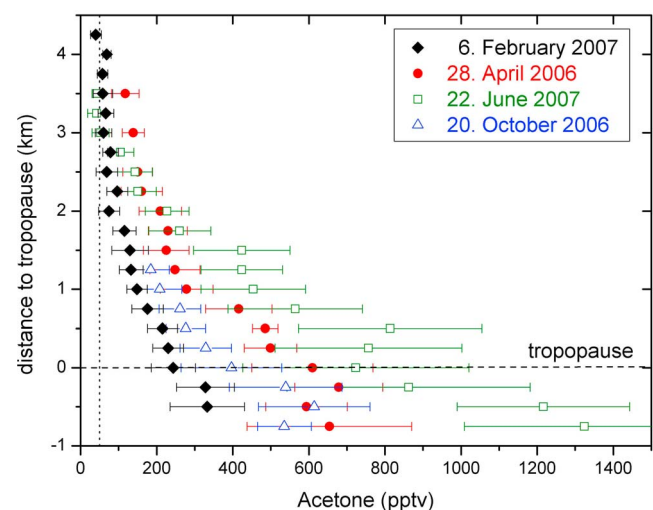


Figure 4. Vertical profile of acetone relative to the tropopause observed during four flights during different seasons. The vertical distance relative to the tropopause is derived from the simultaneously measured O_3 mixing ratio. Horizontal bars indicate 1σ variability.

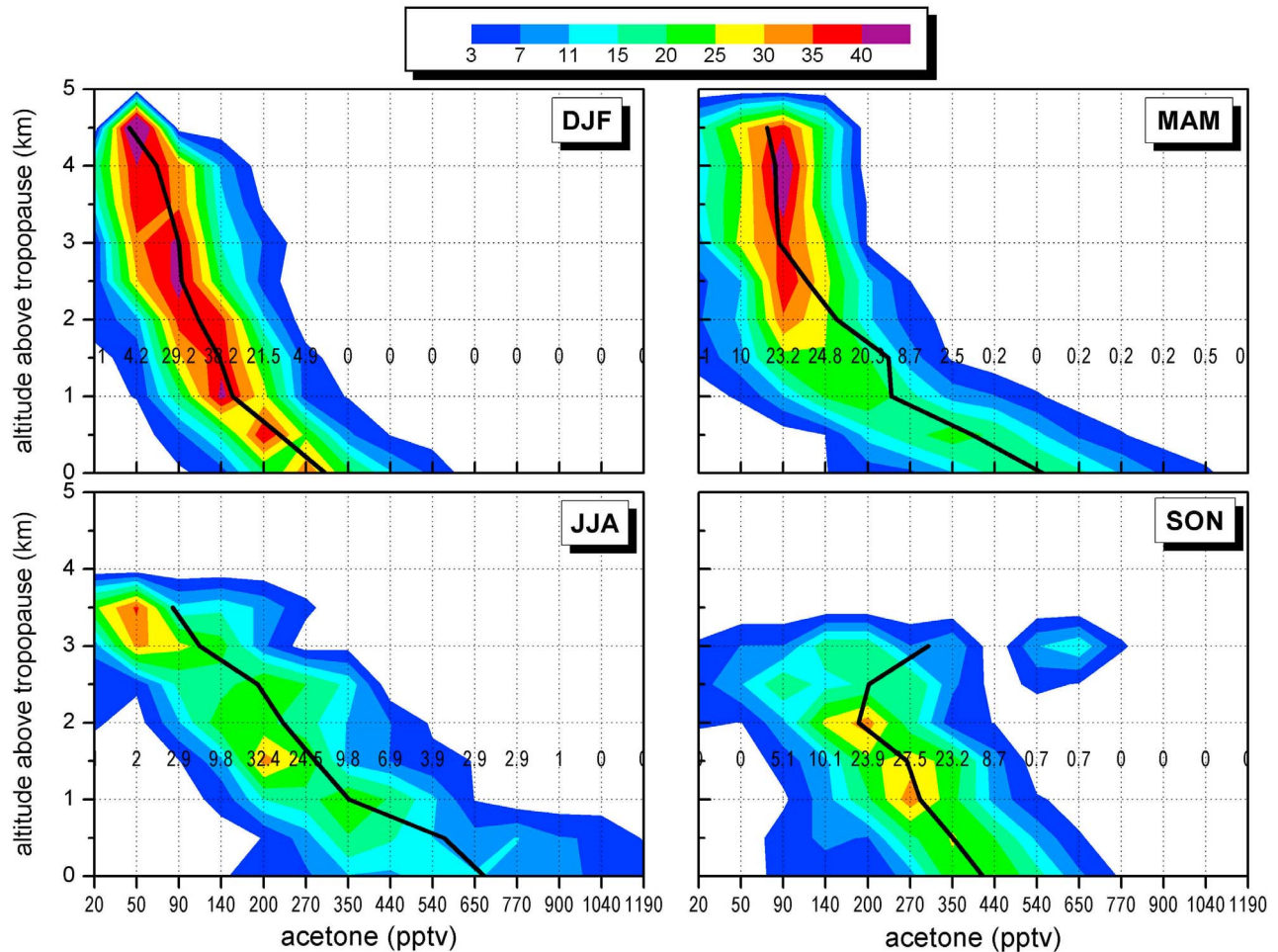


Figure 5. Probability distribution function (PDF) of acetone above the tropopause between 33°N and 56°N and between 200 and 300 hPa during the four seasons. The x axis is not set up in equidistant intervals but shows linearly increasing increments in steps of 10 pptv. Colors indicate the probability of occurrence in percent; each tick on the x axis corresponds to one bin, and the sum of all bins at an altitude level is 100%; as examples, see the percentages at an altitude of 1.5 km above the tropopause. The thick black lines indicate the averaged (mean) profiles.

exclusively originates from atmospheric variability because the instrumental noise due to counting statistics is merely in the 2–5% range of the observed variability. A continuous and gradual decrease of acetone with impressively little fluctuations of the mean values is observed above the tropopause in all flights. These profiles compare very well with the ones observed during the STREAM campaign [Figure 3 in Scheeren *et al.*, 2003]. The transition from UT mixing ratios to the LMS background or to values falling below a lower threshold value of about 50–100 pptv spans the exTL addressed above.

[34] Section 6 will explain that the considerable difference of the acetone profiles above the tropopause depicted in Figure 3 mainly results from a seasonal variation and is not, e.g., caused by short-term differing mixing processes across the tropopause. Before taking on that explanation, we will address the variability of the vertical profile of acetone in more detail.

[35] Figure 5 indicates the probability distribution function (PDF) of acetone relative to the tropopause, based on all flights between February 2006 and December 2008. In

accordance with Figure 4, considerable seasonal variation in the distribution pattern is apparent. Main features are the following.

[36] 1. Acetone bottoms out in winter over the entire altitude range with (arithmetic) mean values of ~ 300 pptv at the tropopause and ~ 50 pptv ~ 4.5 km above it. This demonstrates a minimal in-mixing of tropospheric acetone into the LMS in winter at a time when the chemical lifetime is actually highest. As a consequence, the PDF is most compact and the variability of acetone or tracer flux, respectively, does not imply a minimal (largely reversible) mass flux across the tropopause which, e.g., Sprenger and Wernli [2003] assume to maximize in winter/spring.

[37] 2. Acetone starts to increase just above the tropopause in spring and reaches an altitude of $Z_{\text{TP}}(\text{O}_3) \approx 2.0$ km. This increase continues toward summer with $Z_{\text{TP}}(\text{O}_3)$ reaching 3.0–4.0 km. In summer the vertical gradient of acetone maximizes with, on average, 187 pptv km^{-1} between the tropopause and $Z_{\text{TP}}(\text{O}_3) = 3$ km.

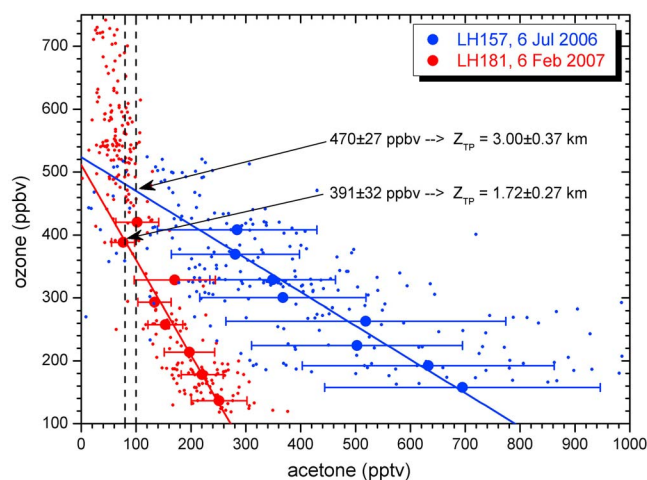


Figure 6. Determination of the Z_{acetone} for a summer and winter flight. Only the stratospheric intersects (one per flight) are shown. The intersection of the linear fit lines with the stratospheric acetone background of 80 pptv (February flight) and 100 pptv (July flight) marks the O_3 mixing ratio at Z_{acetone} .

[38] 3. In autumn the vertical gradient is minimal (see mean vertical profiles), variability is maximal, and elevated mixing ratios of up to ~ 700 pptv occur even 3 km above the tropopause.

[39] The latter finding implies that the chemical contrast across the midlatitude tropopause is minimal in autumn, a finding that agrees with many model studies and observations. Model studies initially by *Chen* [1995], *Eluskiewicz* [1996], and *Dethof et al.* [2000] and thereafter by others [*Berthet et al.* 2007, and references therein] indicate two layers (separated by the isentropic surface of $\Theta \approx 340$ K) that are characterized by quite different seasonal variations of the bidirectional transport across the extratropical tropopause.

[40] In the lower layer between the tropopause and $\Theta \approx 340$ K, vital bidirectional transport occurs throughout the year [*Sprenger and Wernli*, 2003]. This transport pathway, labeled here $\text{STE} < 340\text{K}$, is believed to occur poleward of the subtropical jet and to be the major process that forms the exTL above the extratropical tropopause. The higher-layer $\text{STE} > 340\text{K}$ ($\Theta \approx 340\text{--}370$ K), however, is linked to the subtropical jet and permits significant transport only in summer and early autumn. This transport pathway imports subtropical and tropical air to the LMS largely above the potential temperature surface accessible by passenger aircraft and thus would primarily affect the chemical composition above the exTL, i.e., air that we described as background LMS air. This transport pathway would smooth the contrast of the chemical composition across the midlatitude tropopause and thus would explain (1) the weak vertical gradient of acetone observed in autumn (black line in Figure 5) and (2) the strongly elevated acetone mixing ratios of ~ 700 pptv observed 3 km above the tropopause in autumn (Figure 5). This deep and effective entrainment of tropospheric air into the LMS in summer and early autumn was described by *Ray et al.* [1999], reporting balloon-borne observations of CFC and H_2O at 35°N indicating that the LMS contained 60–90% of tropospheric air in September, but only 10–20% in May. Similar numbers were inferred by more sophisticated mass

balances approaches, e.g., by *Hoor et al.* [2005] and *Bönisch et al.* [2008]. In section 5 we will address in more detail how deep tropospheric acetone is mixed into the LMS.

5. Stratospheric Intrusion Height of Acetone

[41] The dominant source of acetone in the LMS is in-mixing from the upper troposphere. Depending on the chemical lifetime τ_{chem} and the transport time $\tau_{\text{transport}}$ from the UT to the sampling location in the LMS, the intrusion height of a considered trace gas in the LMS will match the top of the dynamically controlled exTL, if τ_{chem} is large compared to $\tau_{\text{transport}}$. However, if $\tau_{\text{chem}} < \tau_{\text{transport}}$ (shorter lived gases) the intrusion height will be at lower altitudes. Acetone constitutes a medium-lived trace gas with minimum lifetime $\tau_{\text{chem, acetone}}$ of about 4 weeks around the summertime midlatitude tropopause (see section 1).

[42] We now address the question how $\tau_{\text{chem, acetone}}$ compares to $\tau_{\text{transport}}$ for establishing how deep acetone can mix into the LMS compared to long-lived species with $\tau_{\text{chem}} \gg \tau_{\text{transport}}$. Here, we define the “stratospheric intrusion height of acetone” Z_{acetone} as a distance above the tropopause at which the linear regression line fitting the vertical gradient of acetone above the tropopause intersects the background concentration of acetone in the LMS. This background value $\text{acetone}_{\text{LMS}}$ is not well-defined by the CARIBIC data. The CARIBIC aircraft sampled background LMS air for a sufficiently long time only 21 times. During the first half of the year, $\text{acetone}_{\text{LMS}}$ averaged 79 pptv ($N = 10$) with small scatter of ~ 20 pptv. During the second half of the year, $\text{acetone}_{\text{LMS}}$ values of ~ 100 pptv were sampled seven times and elevated values of up to 360 pptv (which likely mark in-mixing of tropospheric air at lower latitudes and higher potential temperatures, as discussed in section 4) were sampled four times. We thus consider LMS background concentrations $\text{acetone}_{\text{LMS}}$ to be 80 pptv between January and June and 100 pptv between July and December. The dependence of the inferred acetone intrusion height on the LMS background concentrations $\text{acetone}_{\text{LMS}}$ is $130 \text{ m } 20 \text{ pptv}^{-1}$ (not shown) and thus small compared to the observed variability (see discussion of Figure 7, later).

[43] A program was written that determines Z_{acetone} for each individual transect that reached sufficiently deeply (≥ 1.5 km) into the stratosphere. As an example, the determination of Z_{acetone} is indicated for a typical winter and summer flight in Figure 6. During both flights only one sufficiently strong stratospheric intersect was sampled.

[44] The procedure is that in step 1, the ozone and acetone data for an individual stratospheric intersect, or between the tropopause and a level $\sim 1.5\text{--}2.5$ km above it, respectively, are binned typically in seven to nine bins. In step 2, a linear least squares fit of these averaged data is calculated (straight lines in Figure 6) and its intersection with the acetone background in the LMS of $\text{acetone}_{\text{LMS}} = 80$ pptv or 100 pptv, respectively, is calculated. In the present example ozone mixing ratios are 391 and 470 ppbv for the winter and the summer flights, respectively. Finally, in step 3, this ozone mixing ratio is translated into a height above the tropopause, $Z_{\text{TP}}(\text{O}_3)$ (see section 3 and equation (5)).

[45] Figure 7 gives Z_{acetone} , the O_3 mixing ratio at Z_{acetone} , and the correlation coefficient R for fitting the averaged acetone data between the tropopause and $\sim 1.5\text{--}2.5$ km above

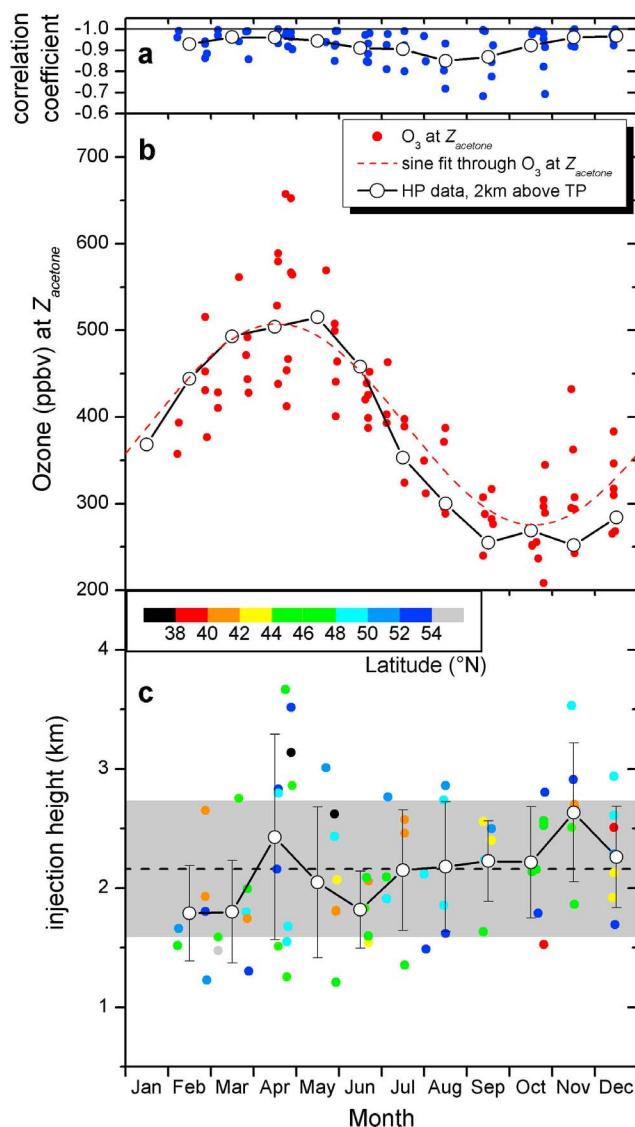


Figure 7. (a) Seasonal variation of the correlation coefficient R between O₃ and acetone inferred just above the tropopause (see Figure 6); blue dots: R for each individual tropopause crossing; dashed line with circles: monthly mean values. (b) Seasonal variation of the O₃ mixing ratio at the stratospheric intrusion height of acetone Z_{acetone} as red dots, a sine fit through these data (dashed red line), and the mean O₃ mixing ratio 2.0 km above the thermal tropopause at the Hohenpeissenberg station (black line with open circles). (c) Seasonal variation of acetone intrusion height Z_{acetone} as colored dots indicating latitude where Z_{acetone} was measured; solid lines connect monthly mean values (open circles); dashed line shows mean Z_{acetone} of 2.16 km; gray area documents 1 σ variability of Z_{acetone} (i.e., 0.57 km).

the tropopause of all 77 individual transects that reached sufficiently deeply into the LMS. The linear correlation coefficient R is very high (Figure 7a), on average $\bar{R} = -0.93 \pm 0.07$ for all 77 profiles. This documents the invariably highly compact negative correlation of ozone with acetone just above the tropopause. Consider, however, that the correlation coefficient is somewhat smaller between August and

October, i.e., just when the vertical gradient of acetone in the LMS minimizes and the variability maximizes (see section 3 and Figure 4).

[46] The ozone mixing ratio at the acetone intrusion height Z_{acetone} (Figure 7b, filled circles) shows a strong seasonal variation, which basically reflects the well-known seasonal variation of ozone in the LMS [Logan, 1999]. In addition to these CARIBIC O₃ data, the mean seasonal variation of ozone observed by ozonesondes 2.0 km above the thermal tropopause over Hohenpeissenberg (47°N, 9°E) between 1967 and 2000 is shown for comparison (line with light circles). These ozonesonde data agree well with the observed ozone levels at the acetone intrusion height Z_{acetone} , which already indicates that the acetone intrusion height Z_{acetone} is about 2 km throughout the year.

[47] Figure 7c shows the acetone intrusion height Z_{acetone} for all 77 individual CARIBIC profiles. A mean value of $Z_{\text{acetone}} = 2.16$ km is derived (1 σ variability, 0.57 km). In winter, Z_{acetone} appears to be somewhat smaller, but the rest of the year the monthly mean values are quite constant (dashed line with open circles). A weak but insignificant increase of Z_{acetone} with latitude was measured, with 2.04 ± 0.47 km at 33–46°N (28 profiles), 2.16 ± 0.62 km at 46–50°N (27 profiles), and 2.31 ± 0.63 km at 50–56°N (22 profiles). This finding could be explained at least partially by the small latitude band in which the CARIBIC aircraft was able to sample air sufficiently far into the LMS and the statistically small number of profiles (77). However, O₃–CO correlations observed by the ACE-FTS instrument onboard Canada’s SCISAT-1, being statistically quite representative, also indicate a very weak latitudinal increase of the vertical extension of the O₃–CO-based exTL Z_{CO} , from ~ 1.8 km at 30°N to ~ 2.2 km at 60°N [Hegglin *et al.*, 2009]. Moreover, these satellite data-derived numbers agree exactly with the acetone intrusion heights (Z_{acetone}) derived in this study. The interpretation of the O₃–CO correlation observed during the CARIBIC I phase from 1997 to 2002 also lets us assume a quite constant vertical depth of the exTL in midlatitudes of 2 km [Zahn *et al.*, 2004].

[48] As Z_{acetone} seems to agree with the vertical depth of the (O₃–CO-based) exTL Z_{CO} , and because the chemical lifetime of acetone is 2–3 times shorter than that of CO, the mean transport time $\tau_{\text{transport}}$ within the exTL cannot be longer than the local chemical lifetime of acetone $\tau_{\text{chem, acetone}}$ of about 4 to 5 weeks in summer.

[49] Orvalez *et al.* [1999] and Hoor *et al.* [2002] suggested that the exTL spans a larger potential temperature range in summer (30–40 K) than in winter (20–25 K). But as the vertical gradient of the potential temperature in the LMS is larger in summer than in winter, and because the statistical significance of the STREAM data studied by Hoor *et al.* [2002] is even lower than of the CARIBIC data interpreted here, we do not see a clear disagreement.

6. Seasonal Variation of Acetone Around the Midlatitude Tropopause

[50] Already Figures 3 and 4 suggest a considerable seasonal variation of acetone in the UT as well as in the LMS. This aspect is brought out more clearly in Figure 8, where the seasonal variation of acetone observed at the tropopause (within an altitude bin of ± 0.25 km around the tropopause,

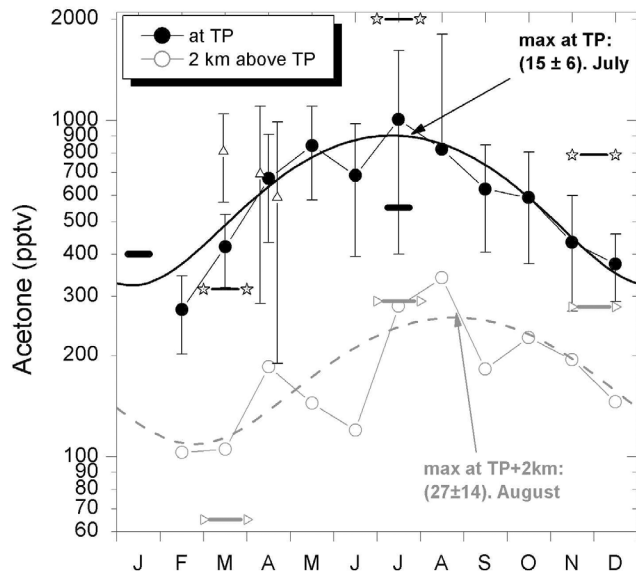


Figure 8. Seasonal variation of acetone at the tropopause (black filled circles) and 2 km above the tropopause (gray open circles) with sine functions that fit the two data sets. Vertical bars indicate 1σ variability. Horizontal black bars with stars, and gray bars with open triangles, indicate observations during the STREAM campaign made at the tropopause and ~ 2 km above it, respectively [Scheeren *et al.*, 2003]. Triangles with error bar in March/April indicate measurements during TRACE-P between 32°N and 40°N in 2001 (measured by H. Singh, available at <http://www-gte.larc.nasa.gov/>). Horizontal black thick bars are model results at the tropopause by Jacob *et al.* [2002].

where again the measured O_3 is interpreted as a vertical scale; see section 3) and 2 km above the tropopause is shown as monthly means with an inferred 1σ variability. In particular, the seasonal variation observed at the tropopause appears very gradually, i.e., is not noisy. This indicates that our data are quite representative, because the considerable atmospheric variability encountered (visualized by the 1σ bars) is already smoothed out. In addition, sine functions that best approximate the monthly mean values are shown as follows:

$$[\text{acetone}]_{\text{TP}} = 613 + 289 \cdot \sin\left(\frac{\text{DOY} - 100}{365} \cdot 2\pi\right) \text{ (in ppbv)} \quad \text{and} \quad (6)$$

$$[\text{acetone}]_{\text{TP}+2\text{km}} = 184 + 75 \cdot \sin\left(\frac{\text{DOY} - 144}{365} \cdot 2\pi\right) \text{ (in ppbv)}, \quad (7)$$

where DOY is day of year.

[51] That is, mean acetone concentrations at the midlatitude tropopause in July (with ~ 900 ppbv) were a factor of ~ 4.5 higher than in January (with ~ 200 ppbv). A similar seasonal variation was found 2 km above the tropopause with a phase shift of $\sim 44 \pm 17$ d and concentrations lower by a factor of ~ 3.3 . If we describe the acetone levels in the exTL as the result of a simple one-way in-mixing from the troposphere, this temporal shift of approximately 6 weeks may be inter-

preted as mean transport time of acetone from the tropopause to an altitude 2 km above it. Consider, however, the large uncertainty of the phase of the inferred sine fits and the respective uncertainty of the phase shift of 17 d. As the trace gas composition of the exTL sampled by CARIBIC is most likely determined only by the shallow transport pathway $\text{STE} < 340\text{K}$, we do not believe that the low-latitude transport pathway $\text{STE} > 340\text{K}$ has significant influence on the inferred phase shift of approximately 6 weeks. See also the discussion on transport pathways and time scales at the end of this section.

[52] In Figure 8 are also plotted aircraft data from incidental aircraft campaigns by Scheeren *et al.* [2003] and during TRACE-P, together with model results by Jacob *et al.* [2002]. The research aircraft data fall in the range of our data (see error bars indicating the 1σ variability encountered during the 3 years of our observations) but are far from being representative. The model results by Jacob *et al.* [2002] give a too weak seasonal variation, values being too low in summer and too high in winter. This comparison underscores the strength of regular long-term observations presented here, which have already provided representative climatologies, at least for trace species with lifetimes at least as long as that of acetone.

[53] The seasonal variation of acetone in the entire altitude range covered by the CARIBIC aircraft is depicted in Figure 9 as a contour plot. As already seen in Figures 3 and 4, the vertical gradient from the UT into the LMS is much stronger in late winter (February/March) than in autumn. Also clearly visible is the continuous and smooth seasonal variation in the UT. In contrast, in the LMS 2.5–3.0 km above the tropopause, acetone seems to undergo a more step-like seasonal change with mixing ratios of 50–100 pptv during the first half of the year and higher values of ~ 200 pptv from July to November, in agreement with Figure 8. Although the statistical significance of this feature may be weak, it agrees with the actual knowledge of the seasonal ventilation of the LMS.

[54] In winter and early spring, the LMS is filled with descending O_3 -rich stratospheric air [Logan, 1999], and in-mixing of UT air occurs only via transport pathway

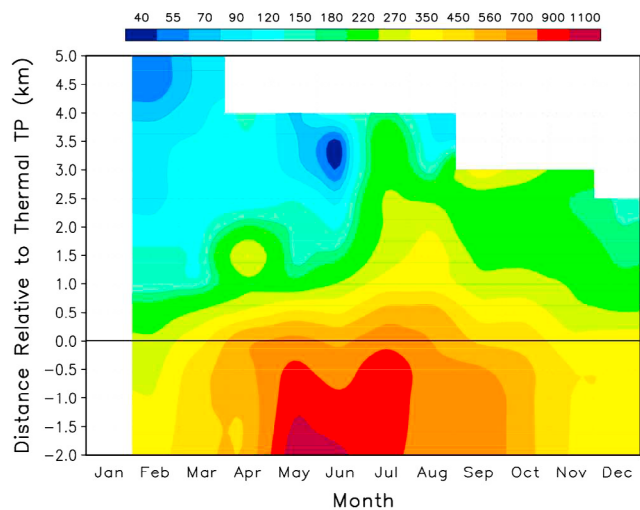


Figure 9. Seasonal variation of acetone (in pptv; see color scale) for a range of distances relative to the thermal tropopause.

STE $<_{340\text{K}}$ (see section 4): that is, the in-mixing is both shallow and restricted to the first ~ 2 km or ~ 25 K in potential temperature above the tropopause [Hoor *et al.*, 2004; Zahn *et al.*, 2004; Pan *et al.*, 2004; Hegglin *et al.*, 2006, 2009]. In summer and early autumn the tropopause becomes additionally permeable near the subtropical jet stream via STE $>_{340\text{K}}$ (see section 4), which allows in-mixing of UT air into the LMS at higher altitudes or at higher potential temperatures. For instance, in October Ray *et al.* [1999] observed CFC concentrations in the entire LMS that were indicative for tropospheric air. The transition to the low stratospheric values was encountered only at the LMS upper boundary, i.e., at pressures of ~ 100 hPa or at ~ 380 K. In contrast, in May this transition was observed at much lower altitudes, namely, at the LMS lower boundary, the tropopause. A mass balance approach by Bönisch *et al.* [2008] applied to aircraft data collected during the SPURT campaigns likewise suggests the proportion of tropospheric air in the LMS is 80% during October, but below 20% in April. Also the excellent paper by Sawa *et al.* [2008] on the seasonal variation of CO₂ in the UT/LMS based on observations onboard passenger aircraft describes the change in the ventilation of the LMS in summer [see, e.g., Figure 9 by Sawa *et al.*, 2008].

[55] In summer a larger fraction of acetone may actually reach altitudes of more than 2 km higher above the tropopause than in autumn, but this decreasing flux of acetone may be counterbalanced by two processes: (1) the rapidly increasing lifetime of acetone of approximately 4 weeks in July compared with a lifetime of approximately 10 weeks in October [Arnold *et al.*, 2005] and (2) the transport pathway STE $>_{340\text{K}}$ around the subtropical jet, which is active only in summer and early autumn. Because of the phase shift between transport flux and a subsequently changing mixing ratio and the increasing chemical lifetime, this transport pathway STE $>_{340\text{K}}$ may lead to elevated acetone levels at the CARIBIC sampling latitudes north of $\sim 35^\circ\text{N}$ in autumn. Both processes together may lead to observation of quite constant acetone concentrations between July and November (when the subsidence of O₃-rich stratospheric air reaches this altitude range).

[56] Indeed, a few studies interpreting the seasonal cycle of CO₂ in the LMS conclude that this low-latitude transport channel STE $>_{340\text{K}}$ significantly influences the trace gas composition of the background LMS [Nakazawa *et al.*, 1991; Boering *et al.*, 1995, 1996; Strahan *et al.*, 2007; Hoor *et al.*, 2004; Gurk *et al.*, 2008; Sawa *et al.*, 2008]. Our evaluations imply that only the data from the LMS background (>2.5 km in Figures 5 and 9) are influenced by the transport pathway STE $>_{340\text{K}}$, not the data from the exTL.

7. Conclusions

[57] The regular monitoring of acetone onboard the CARIBIC passenger aircraft since May 2005 has led to an impressive data set for the midlatitude UT and LMS. It constitutes the most representative data set so far of acetone from the UT/LMS.

[58] A gradual but strong seasonal variation was observed with maximal mixing ratios of $\sim 900(270)$ pptv in summer and minimal values of $\sim 200(100)$ pptv in winter at the tropopause (2 km above it). In combination with ozonesonde data from 12 stations north of 35°N , the CARIBIC ozone data were

translated to a vertical distance above the tropopause with a high accuracy of $\sim 20\%$ (Table 1). This enabled us to retrieve accurate seasonal variations relative to the tropopause and to quantify the transport times of in-mixing tropospheric air from the tropopause to certain altitudes in the LMS. The vertically progressively increasing phase shift of the seasonal variation let us estimate mean transport times of about 6 weeks from the tropopause to an altitude 2 km above it.

[59] Acetone and ozone were always strongly negatively correlated in the LMS, with an average correlation coefficient of -0.93 for all 77 intersects that reached sufficiently deeply (>1.5 km) into the stratosphere. This anticorrelation is caused by the mixing of inflowing tropospheric air and subsiding stratospheric air within the extratropical tropopause mixing layer (exTL). The vertical extension of the (O₃-acetone-based) exTL was quantified as ~ 2.0 km throughout the year, which agrees nicely with the first satellite-based view of the exTL based on the correlation of O₃ and CO [Hegglin *et al.*, 2009].

[60] PDFs of acetone for the four seasons and the seasonal variation of acetone relative to the tropopause as a contour plot were used to identify the processes that determine the in-mixing and subsequent dispersion of acetone in the LMS. In winter this in-mixing was shallow and led, in spite of the then maximum chemical lifetimes, to low acetone levels (~ 50 pptv) 2–5 km above the tropopause. In summer, stronger and deeper in-mixing was ascertained that, together with the increasing chemical lifetimes and additional poleward transport of acetone injected into the LMS at lower latitudes, resulted in quite constant acetone levels in the LMS until November.

[61] A more extensive analysis of the tropospheric acetone data in combination with other trace gases measured by the PTR-MS and other instruments in the CARIBIC container is in progress.

[62] **Acknowledgments.** We are very grateful to Carl Brenninkmeijer (Max-Planck-Institute for Chemistry, Mainz) for his contagious enthusiasm and excellent review of the manuscript. We also thank Dieter Scharffe, Claus Köppel, Franz Slemr, and Tanja Schuck (same institute) for servicing the complex CARIBIC container and for conducting all the time-consuming ground tests to guarantee accurate measurements at flight. We thank J. Logan (Harvard University) for providing the O₃ sonde data used to derive the vertical altitude above the tropopause. We acknowledge the support of the European Commission through the GEOmon (Global Earth Observation and Monitoring) Integrated Project under the 6th Framework Program (contract FP6-2005-Global-4-036677).

References

- Appenzeller, C., H. C. Davies, and W. A. Norton (1996), Fragmentation of stratospheric intrusions, *J. Geophys. Res.*, *101*, 1435–1456, doi:10.1029/95JD02674
- Arnold, F., and G. Hauck (1985), Lower stratosphere trace gas detection using aircraft-borne active chemical ionization mass spectrometry, *Nature*, *315*, 307–309, doi:10.1038/315307a0.
- Arnold, F., G. Knop, and H. Ziereis (1986), Acetone measurements in the upper troposphere and lower stratosphere—Implications for hydroxyl radical abundances, *Nature*, *321*, 505–507, doi:10.1038/321505a0.
- Arnold, F., V. Buerger, B. Droste-Franke, F. Grimm, A. Krieger, J. Schneider, and T. Stipl (1997), Acetone in the upper troposphere and lower stratosphere: Impact on trace gases and aerosols, *Geophys. Res. Lett.*, *24*, 3017–3020, doi:10.1029/97GL02974.
- Arnold, S. R., M. P. Chipperfield, M. A. Blitz, D. E. Heard, and M. J. Pilling (2004), Photodissociation of acetone: Atmospheric implications of temperature-dependent quantum yields, *Geophys. Res. Lett.*, *31*, L07110, doi:10.1029/2003GL019099.

- Arnold, S. R., M. P. Chipperfield, and M. A. Blitz (2005), A three-dimensional model study of the effect of new temperature-dependent quantum yields for acetone photolysis, *J. Geophys. Res.*, *110*, D22305, doi:10.1029/2005JD005998.
- Berthet, G., J. G. Esler, and P. H. Haynes (2007), A Lagrangian perspective of the tropopause and the ventilation of the lowermost stratosphere, *J. Geophys. Res.*, *112*, D18102, doi:10.1029/2006JD008295.
- Blitz, M. A., D. E. Heard, M. J. Pilling, S. R. Arnold, and M. P. Chipperfield (2004), Pressure and temperature-dependent quantum yields for the photodissociation of acetone between 279 and 327.5 nm, *Geophys. Res. Lett.*, *31*, L06111, doi:10.1029/2003GL018793.
- Boering, K. A., et al. (1995), Measurements of stratospheric carbon dioxide and water vapor at northern midlatitudes: Implications for troposphere-to-stratosphere transport, *Geophys. Res. Lett.*, *22*, 2737–2740, doi:10.1029/95GL02337.
- Boering, K. A., S. C. Wofsy, B. C. Daube, J. R. Schneider, M. Loewenstein, J. R. Podolske, and T. J. Conway (1996), Stratospheric mean ages and transport rates from observations of CO₂ and N₂O, *Science*, *274*, 1340–1343, doi:10.1126/science.274.5291.1340.
- Bönisch, H., A. Engel, J. Curtius, T. Birner, and P. Hoor (2008), Quantifying transport into the lowermost stratosphere using simultaneous in-situ measurements of SF₆ and CO₂, *Atmos. Chem. Phys. Discuss.*, *8*, 21,229–21,264, doi:10.5194/acpd-8-21229-2008.
- Brenninkmeijer, C. A. M., et al. (2005), Analyzing atmospheric trace gases and aerosols using passenger aircraft, *Eos Trans. AGU*, *86*(8), 77–88, doi:10.1029/2005EO080001.
- Brenninkmeijer, C. A. M., et al. (2007), Civil aircraft for the regular investigation of the atmosphere based on an instrument container: The new CARIBIC system, *Atmos. Chem. Phys.*, *7*, 4953–4976, doi:10.5194/acp-7-4953-2007.
- Butchart, N., and E. E. Remsburg (1986), The area of the stratospheric polar vortex as a diagnostic tracer for transport on an isentropic surface, *J. Atmos. Sci.*, *43*, 1319–1339, doi:10.1175/1520-0469(1986)043<1319:TAOTSP>2.0.CO;2.
- Chatfield, B., E. P. Gardener, and J. G. Calvert (1987), Sources and sinks of acetone in the troposphere: Behavior of reactive hydrocarbons and a stable product, *J. Geophys. Res.*, *92*, 4208–4216, doi:10.1029/JD092iD04p04208.
- Chen, P. (1995), Isentropic cross-tropopause mass exchange in the extratropics, *J. Geophys. Res.*, *100*, 16,661–16,673.
- Coheur, P.-F., et al. (2007), ACE-FTS observation of a young biomass burning plume: First reported measurements of C₂H₄, C₃H₆O, H₂CO and PAN by infrared occultation from space, *Atmos. Chem. Phys.*, *7*, 5437–5446, doi:10.5194/acp-7-5437-2007.
- Colomb, A., et al. (2006), Airborne measurements of trace organic species in the upper troposphere over Europe: The impact of deep convection, *Environ. Chem.*, *3*(4), 244–259, doi:10.1071/EN06020.
- Considine, D. B., J. A. Logan, and M. A. Olsen (2008), Evaluation of near-tropopause ozone distributions in the Global Modeling Initiative combined stratosphere/troposphere model with ozonesonde data, *Atmos. Chem. Phys.*, *8*, 2365–2385, doi:10.5194/acp-8-2365-2008.
- Cours, T., S. Canneaux, and F. Bohr (2007), Features of the potential energy surface for the reaction of HO₂ radical with acetone, *Int. J. Quantum Chem.*, *107*, 1344–1354, doi:10.1002/qua.21269.
- de Gouw, J., and C. Warneke (2007), Measurements of volatile organic compounds in the Earth's atmosphere using proton-transfer-reaction mass spectrometry, *Mass Spectrom. Rev.*, *26*, 223–257.
- de Gouw, J., C. Warneke, R. Holzinger, T. Kluepfel, and J. Williams (2004), Inter-comparison, between airborne measurements of methanol, acetonitrile and acetone using two differently configured PTR-MS instruments, *Int. J. Mass Spectrom.*, *239*, 129–137, doi:10.1016/j.ijms.2004.07.025.
- de Laat, A. T. J., J. A. de Gouw, J. Lelieveld, and A. Hansel (2001), Model analysis of trace gas measurements and pollution impact during INDOEX, *J. Geophys. Res.*, *106*(D22), 28,469–28,480, doi:10.1029/2000JD900821.
- Dethof, A., A. O'Neill, and J. Slingo (2000), Quantification of isentropic mass transport across the dynamical tropopause, *J. Geophys. Res.*, *105*, 12,279–12,293.
- Eluszkiewicz, J. (1996), A three-dimensional view of the stratosphere-to-troposphere exchange in the GFDL SKYHI model, *Geophys. Res. Lett.*, *23*, 2489–2492, doi:10.1029/96GL02262.
- Fischer, H., F. G. Wienhold, P. Hoor, O. Bujok, C. Schiller, P. Siegmund, M. Ambaum, H. A. Scheeren, and J. Lelieveld (2000), Tracer correlations in the northern high latitude lowermost stratosphere: Influence and cross-tropopause mass exchange, *Geophys. Res. Lett.*, *27*, 97–100, doi:10.1029/1999GL010879.
- Fischer, H., et al. (2003), Deep convective injection of boundary layer air into the lowermost stratosphere at midlatitudes, *Atmos. Chem. Phys.*, *3*, 739–745, doi:10.5194/acp-3-739-2003.
- Folkins, I., R. Chartfield, H. Singh, Y. Chen, and B. Heikes (1998), Ozone production efficiencies of acetone and peroxides in the upper troposphere, *Geophys. Res. Lett.*, *25*, 1305–1308, doi:10.1029/98GL01030.
- Gurk, C., H. Fischer, P. Hoor, M. G. Lawrence, J. Lelieveld, and H. Wernli (2008), Airborne in-situ measurements of vertical, seasonal and latitudinal distributions of carbon dioxide over Europe, *Atmos. Chem. Phys.*, *8*, 6395–6403, doi:10.5194/acp-8-6395-2008.
- Hansel, A., A. Jordan, C. Warneke, R. Holzinger, A. Wisthaler, and W. Lindinger (1998), Improved detection limit of the proton-transfer reaction mass spectrometer: On-line monitoring of volatile organic compounds at mixing ratios of a few pptv, *Rapid Commun. Mass Spectrom.*, *12*, 871–875, doi:10.1002/(SICI)1097-0231(19980715)12:13<871::AID-RCM245>3.0.CO;2-L.
- Hegglin, M. I., D. Brunner, T. Peter, P. Hoor, H. Fischer, J. Staehelin, M. Krebssbach, C. Schiller, U. Parchatka, and U. Weers (2006), Measurements of NO, NO₂, N₂O, and O₃ during SPURT: Implications for transport and chemistry in the lowermost stratosphere, *Atmos. Chem. Phys.*, *6*, 1331–1350, doi:10.5194/acp-6-1331-2006.
- Hegglin, M. I., C. D. Bonne, G. L. Manney, and K. A. Walker (2009), A global view of the extratropical tropopause transition layer from Atmospheric Chemistry Experiment Fourier Transform Spectrometer O₃, H₂O, and CO, *J. Geophys. Res.*, *114*, D00B11, doi:10.1029/2008JD009984.
- Hermans, I., T. L. Nguyen, P. A. Jacobs, and J. Peeters (2004), Tropopause chemistry revisited: HO₂-initiated oxidation as an efficient acetone sink, *J. Am. Chem. Soc.*, *126*, 9908–9909, doi:10.1021/ja0467317.
- Hermans, I., J.-F. Müller, and T. L. Nguyen, P. A. Jacobs, and J. Peeters (2005), Kinetics of α -hydroxy-alkylperoxy radicals in oxidation processes. HO₂-initiated oxidation of ketones/aldehydes near the tropopause, *J. Phys. Chem. A*, *109*, 4303–4311, doi:10.1021/jp044080v.
- Holton, J. R., P. H. Haynes, M. E. McIntyre, A. R. Douglass, R. B. Rood, and L. Pfister (1995), Stratosphere-troposphere exchange, *Rev. Geophys.*, *33*, 403–439, doi:10.1029/95RG02097.
- Hoor, P., H. Fischer, L. Lange, J. Lelieveld, and D. Brunner (2002), Seasonal variations of a mixing layer in the lowermost stratosphere as identified by the CO–O₃ correlation from in situ measurements, *J. Geophys. Res.*, *107*(D5), 4044, doi:10.1029/2000JD000289.
- Hoor, P., C. Gurk, D. Brunner, M. I. Hegglin, H. Wernli, and H. Fischer (2004), Seasonality and extent of extratropical TST derived from in-situ measurements during SPURT, *Atmos. Chem. Phys.*, *4*, 1427–1442, doi:10.5194/acp-4-1427-2004.
- Hoor, P., H. Fischer, and J. Lelieveld (2005), Tropical and extratropical tropospheric air in the lowermost stratosphere over Europe: A CO-based budget, *Geophys. Res. Lett.*, *32*, L07802, doi:10.1029/2004GL020218.
- Jacob, D. J., et al. (1996), Origin of ozone and NO_x in the tropical troposphere; A photochemical analysis of aircraft observations over the South Atlantic Basin, *J. Geophys. Res.*, *101*, 24,235–24,250, doi:10.1029/96JD00336.
- Jacob, D. J., B. D. Field, E. M. Jin, I. Bey, Q. B. Li, J. A. Logan, R. M. Yantosca, and H. B. Singh (2002), Atmospheric budget of acetone, *J. Geophys. Res.*, *107*(D10), 4100, doi:10.1029/2001JD000694.
- Jaeglé, L., et al. (1997), Observations of OH and HO₂ in the upper troposphere suggest a strong source from convective injection of peroxides, *Geophys. Res. Lett.*, *24*, 3181–3184, doi:10.1029/97GL03004.
- Jaeglé, L., D. J. Jacob, W. H. Brune, and P. O. Wennberg (2001), Chemistry of HO_x radicals in the upper troposphere, *Atmos. Environ.*, *35*, 469–489, doi:10.1016/S1352-2310(00)00376-9.
- Kiendler, A., and F. Arnold (2003), Detection of gaseous oxygenated hydrocarbons in upper tropospheric and lower stratospheric aircraft borne experiments, *Int. J. Mass Spectrom.*, *223–224*, 733–741, doi:10.1016/S1387-3806(02)00969-7.
- Lindinger, W., A. Hansel, and A. Jordan (1998), On-line monitoring of volatile organic compounds at ppt levels by means of proton-transfer-reaction mass spectrometry (PTR-MS) Medical applications, food control and environmental research, *Int. J. Mass Spectrom. Ion Process.*, *173*, 191–241, doi:10.1016/S0168-1176(97)00281-4.
- Logan, J. A. (1999), An analysis of ozonesonde data for the lower stratosphere: Recommendations for testing models, *J. Geophys. Res.*, *104*, 16,151–16,170, doi:10.1029/1999JD900216.
- Nakazawa, T., K. Miyashita, S. Aoki, and M. Tanaka (1991), Temporal and spatial variations of upper tropospheric and lower stratospheric carbon dioxide, *Tellus, Ser. B*, *43*, 106–117, doi:10.1034/j.1600-0889.1991.t011-1-00005.x.
- Orvaldez, J., P. van Velthoven, and H. Schlager (1999), Water vapor measurements from the troposphere to the lowermost stratosphere: Some signatures of troposphere to stratosphere exchanges, *J. Geophys. Res.*, *104*, 16,673–16,678.
- Pan, L. L., W. J. Randel, B. L. Gary, M. J. Mahoney, and E. J. Hints (2004), Definitions and sharpness of the extratropical tropopause: A trace

- gas perspective, *J. Geophys. Res.*, *109*, D23103, doi:10.1029/2004JD004982.
- Ray, E. A., F. L. Moore, J. W. Elkins, G. S. Dutton, D. W. Fahey, H. Vömel, S. J. Oltmans, and K. H. Rosenlof (1999), Transport into the Northern Hemisphere lowermost stratosphere revealed by in situ tracer measurements, *J. Geophys. Res.*, *104*, 26,565–26,580, doi:10.1029/1999JD900323.
- Reid, S. J., and G. Vaughan (1991), Lamination in ozone profiles in the lower stratosphere, *Q. J. R. Meteorol. Soc.*, *117*, 825–844, doi:10.1002/qj.49711750009.
- Remedios, J. J., G. Allen, A. M. Waterfall, H. Oelhaf, A. Kleinert, and D. P. Moore (2007), Detection of organic compound signatures in infra-red, limb emission spectra observed by the MIPAS-B2 balloon instrument, *Atmos. Chem. Phys.*, *7*, 1599–1613, doi:10.5194/acp-7-1599-2007.
- Sawa, Y., T. Machida, and H. Matsueda (2008), Seasonal variations of CO₂ near the tropopause observed by commercial aircraft, *J. Geophys. Res.*, *113*, D23301, doi:10.1029/2008JD010568.
- Scheeren, H. A., et al. (2003), Reactive organic species in the northern extratropical lowermost stratosphere: Seasonal variability and implications for OH, *J. Geophys. Res.*, *108*(D24), 4805, doi:10.1029/2003JD003650.
- Singh, H. B., et al. (1994), Acetone in the atmosphere: Distribution, sources and sinks, *J. Geophys. Res.*, *99*, 1805–1819, doi:10.1029/93JD00764.
- Singh, H. B., M. Kanakidou, P. J. Crutzen, and D. J. Jacob (1995), High concentrations and photochemical fate of oxygenated hydrocarbons in the global troposphere, *Nature*, *378*, 50–54, doi:10.1038/378050a0.
- Singh, H. B., Y. Chen, G. L. Gregory, G. W. Sachse, R. Talbot, D. R. Blake, Y. Kondo, J. D. Bradshaw, B. Heikes, and D. Thornton (1997), Trace chemical measurements from the northern midlatitude lowermost stratosphere in early spring: Distributions, correlations, and fate, *Geophys. Res. Lett.*, *24*, 127–130, doi:10.1029/96GL03770.
- Singh, H. B., et al. (2000), Distribution and fate of selected organic species in the troposphere and lower stratosphere over the Atlantic, *J. Geophys. Res.*, *105*, 3795–3805, doi:10.1029/1999JD900779.
- Singh, H. B., Y. Chen, A. Staudt, D. Jacob, D. Blake, B. Heikes, and J. Snow (2001), Evidence from the Pacific troposphere for large global sources of oxygenated organic compounds, *Nature*, *410*, 1078–1081, doi:10.1038/35074067.
- Singh, H. B., A. Tabazadeh, M. J. Evans, B. D. Field, D. J. Jacob, G. Sachse, J. H. Crawford, R. Shetter, and W. H. Brune (2003), Oxygenated volatile organic chemicals in the oceans: Interferences and implications based on atmospheric observations and air-sea exchange models, *Geophys. Res. Lett.*, *30*(16), 1862, doi:10.1029/2003GL017933.
- Singh, H. B., et al. (2004), Analysis of the atmospheric distribution, sources, and sinks of oxygenated volatile organic chemicals based on measurements over the Pacific during TRACE-P, *J. Geophys. Res.*, *109*, D15S07, doi:10.1029/2003JD003883.
- Solomon, S., R. R. Garcia, and F. Stordal (1985), Transport processes and ozone perturbations, *J. Geophys. Res.*, *90*, 12,981–12,989.
- Sprenger, M., and H. Wernli (2003), A Northern Hemispheric climatology of cross-tropopause exchange for the ERA15 time period (1979–1993), *J. Geophys. Res.*, *108*(D12), 8521, doi:10.1029/2002JD002636.
- Strahan, S. E., B. N. Duncan, and P. Hoor (2007), Observationally derived transport diagnostics for the lowermost stratosphere and their application to the GMI chemistry and transport model, *Atmos. Chem. Phys.*, *7*, 2435–2445, doi:10.5194/acp-7-2435-2007.
- Thouret, V., J.-P. Cammas, B. Sauvage, G. Athier, R. Zbinden, P. Nédélec, P. Simon, and F. Karcher (2006), Tropopause referenced ozone climatology and inter-annual variability (1994–2003) from the MOZAIC programme, *Atmos. Chem. Phys.*, *6*, 1033–1051, doi:10.5194/acp-6-1033-2006.
- Warneke, C., and J. A. de Gouw (2001), Organic trace gas composition of the marine boundary layer over the northwest Indian Ocean in April 2000, *Atmos. Environ.*, *35*, 5923–5933, doi:10.1016/S1352-2310(01)00384-3.
- Wennberg, P. O., et al. (1998), Hydrogen radicals, nitrogen radicals, and the production of O₃ in the upper troposphere, *Science*, *279*, 49–53, doi:10.1126/science.279.5347.49.
- Williams, J., U. Pöschl, P. J. Crutzen, A. Hansel, R. Holzinger, C. Warneke, W. Lindinger, and J. Lelieveld (2001), An atmospheric chemistry interpretation of mass scans obtained from a proton transfer mass spectrometer flown over the tropical rainforest of Surinam, *J. Atmos. Chem.*, *38*, 133–166, doi:10.1023/A:1006322701523.
- Wisthaler, A., A. Hansel, R. R. Dickerson, and P. J. Crutzen (2002), Organic trace gas measurements by PTR-MS during INDOEX 1999, *J. Geophys. Res.*, *107*(D19), 8024, doi:10.1029/2001JD000576.
- Wohlfrom, K. H., T. Hauler, F. Arnold, and H. Singh (1999), Acetone in the free troposphere and lower stratosphere: Aircraft-based CIMS and GC measurements over the North Atlantic and first comparison, *Geophys. Res. Lett.*, *26*, 2849–2852, doi:10.1029/1999GL900597.
- Zahn, A., C. A. M. Brenninkmeijer, and P. F. J. van Velthoven (2004), Passenger aircraft project CARIBIC 1997–2002, Part II: The ventilation of the lowermost stratosphere, *Atmos. Chem. Phys. Discuss.*, *4*, 1119–1150, doi:10.5194/acpd-4-1119-2004.

D. Sprung and A. Zahn, Karlsruhe Institute of Technology (KIT), Institute of Meteorology and Climate, P.O. Box 3640, Karlsruhe, D-76021, Germany. (andreas.zahn@kit.edu)